

## A 5 cm Bore SSC Dipole Design with Increased Operating Margin

C. Taylor, C. Peters, and S. Caspi

We have recently made a conceptual design suitable for the SSC main collider dipole but with a 5 cm coil bore instead of the present 4 cm bore; in addition, to have a design that will achieve 6.6T with greater reliability and less training, we have increased the number of superconducting strands in each cable by about 20%.

Other features of the design that we believe represent improvements are:

- a) vertical split in the iron yoke
- b) use of a "spacer bar" to precisely to control the air gap in the yoke at assembly and during cooldown
- c) symmetrical, interlocking collar design

These features could well be introduced into the present 4 cm SSC dipole if desired. Features a) and b) were used in a previous 5 cm 9T conceptual design for another application<sup>1)</sup>; the vertical yoke split has been used before (for example, the HERA dipole) Feature c) has recently been proposed as an improvement to the present 4 cm design.

Fig. 1 shows a cross-section of the proposed design. This report describes the design and its main features: cable, coil cross-section, field uniformity, collar design, and yoke/shell design. A brief comparison of the 5-cm cross-section with the present 4 cm design is made from which an approximate cost comparison can be made.

### Cable

The present 4 cm SSC dipole design has a narrow margin between the operating current at  $B_0 = 6.6T$  and the plateau or "short-sample" current. For the present cable specifications, assuming a Cu/SC ratio of 1.3 for the inner cable, the operating current is 6.50KA and the theoretical "short sample" current (along the "load line") is 6.79KA at  $B_0=6.86T$ , a 4.5% margin. (See Appendix I). This "margin" has to accommodate a number of practical operating conditions including:

- a) possible failure to achieve "short sample" current with little or no training.
- b) quality variation within the cable lengths (only the ends are tested).
- c) cable damage, if any, caused by coil fabrication process.
- d) unpredicted local fluctuations in operating temperature.

We cannot rely on further increase in critical current density of the NbTi alloy (although we are actively pursuing this in R&D trials). Therefore, to achieve significantly greater operating margin, the operating temperature will have to be reduced, and/or additional NbTi incorporated into the coils by increasing the width of the cable. (The foregoing assumes that we cannot reliably increase the NbTi cross-section by simply reducing the Cu/SC ratio because of quench protection and stability).

We propose to increase the number of strands in the inner cable from 23 to 28 (increase by 1.22) and in the outer cable from 30 to 36 (increase by 1.20); the strand diameter and Cu/SC ratio remain unchanged so these changes can easily be incorporated without changing the present strand specification or the cabling methods. Cables up to 36 strands have reliably been made reliably with strand diameter of .020 in. (a more difficult task than with the proposed larger strand).

Table 1 compares the proposed cable and the present SSC cable.

	Present SSC Cable	Proposed "wide" SSC Cable
<b>Inner</b>		
Strand Diameter	0.0318 in.	0.0318 in.
Cu/SC ratio	1.3	1.3
Filament diameter	6 μm	6μm
Twist	1-2 per in.	1-2 per in.
Number strands	23	28
Keystone angle	1.6 deg.	1.32 deg.
Thickness	0.0523/0.0625 in.	0.0523/0.0625 in.
Width	0.366 in.	0.446 in.
<b>Outer</b>		
Strand Diameter	.0255 in.	.0255i n.
Cu/SC ratio	1.8	1.8
Filament diameter	6 μm	6μm
Twist	1-2 per in.	1-2 per in.
Number strands	30	36
Keystone angle	1.2 deg.	1.01 deg.
Thickness	0.0418/0.0499 in.	0.0418/0.0499 in.
Width	0.383 in.	0.460 in.

Note that the cable mid-thickness remains unchanged; only the width and thus the keystone angle are changed. Therefore, the degree of compaction at both inner and outer edge is unchanged and cable degradation should be unchanged. The same insulation thickness as in the present design is assumed throughout.

### Coil Design

Because of the increased bore, the number of turns per coil is increased from 16 to 19 for the inner layer and from 20 to 24 for the outer layer. A coil cross-section design that gives a very uniform field is shown in Fig. 2. This design with 3 inner wedges and one outer wedge per quadrant (as in the present design) gives unusually low calculated multipoles as given in Table II, at a reference radius of 1.25 cm. (For the 4 cm design, the reference radius generally used is 1.0 cm)

Table II Harmonics at  $r = 1.25$  cm

Harmonic	$b_n = B_0/B_n$
6 - pole, $b_2$	$.0003 \times 10^{-4}$
10 - pole, $b_4$	$.0002 \times 10^{-4}$
14 - pole, $b_6$	$.0015 \times 10^{-4}$
18 - pole, $b_8$	$.0024 \times 10^{-4}$

Iron saturation effects at  $r = 1.25$  cm should be similar to those for the present 4 cm design at  $r = 1.0$  cm.

For  $\mu = \infty$  iron, the calculated operating current is 6652A for  $B_0 = 6.6$ T. Operating current will be slightly 4% higher for "real" iron, about 6770A. (See Appendix A). Peak magnetic field at the pole turn, is 6.9T for the inner layer and 5.66T for the outer layer; these values are very similar to those of the present design; however, the inner cable now has 1.22 times more superconductor and therefore has a much greater design "margin". The outer cable has a similarly increased "margin". The current "margin", calculated "along the load line", is 12.1% vs 4.5% for the present design, an increase of 2.7; details of this calculation are given in Appendix A.

### Collar Design

The collar pack has two part symmetrical, interlocking collars as shown in Fig. 1. Collar thickness of 20 mm was selected to give slightly lower collar stresses than the present 15 mm design and increased stiffness; this might be reduced with optimization. A symmetrical two-piece collar of somewhat similar geometry, but without interlocking between opposing collars, was used in an earlier CERN dipole<sup>4</sup>); the interlocking design is much more rigid. This approach was used

earlier in quadrupole collar packs at LBL<sup>3</sup>). The outside profile will be circular. Tapered keys (approx. 0.3" x .25") similar to those which have worked well in the NC9 SSC dipole collar design will be used. The symmetrical design reduces pin shear loads to about half those existing in the present pinned collar design. During magnet excitation the horizontal coil forces are resisted by a rigid unjointed collar lamination as opposed to a two piece collar with a pinned (or spot welded) joint in the present case.

Aluminum is proposed because of a) its greater thermal contraction and resulting lower loss of prestress with cooldown and b) lower cost. Since the Lorentz forces are supported by the yoke, the stiffness of Aluminum is adequate; however, all of the other features of the design would be very similar for an identical collar of stainless steel.

### Yoke Design

The iron cross-section at the midplane is increased approx. 20% to accommodate the magnetic flux of the larger bore. Other requirements of the yoke assembly are to carry helium coolant flow, high current busses, correction coil leads, and warm-up heaters; Fig. 1 shows some of these features; although the yoke has not yet been analyzed magnetically, there appears to be sufficient space near the pole regions to accommodate the same services as in the present yoke.

The changes in radial thickness of the main magnet components are listed in Table III.

Table III - radial thickness of major components

	Proposed 5 cm Design		Present 4 cm Design	
	mm	inches	mm	inches
Bore radius	25.0	0.984	20.0	0.787
Cable (2 layers)	23.67	0.932	19.68	0.775
Collar	20.0	0.787	15.0	0.590
Iron	93.72	3.69	77.47	3.05
Shell	7.92	0.312	4.77	0.188
Total radius	170.32	6.71	136.93	5.391
Radius increase	33.39	1.315		
Dia. increase	66.78	2.629		

Shell thickness was chosen to be 0.312 in. (5/16); although simple scaling would give only a 20% increase to 0.226 in., we judge that the greater shell thickness is desirable for proper yoke clamping under all conditions.

The resulting overall increase in the cold mass O.D. is 2.63 in.

In addition to the slightly large yoke needed to accommodate the flux, several other features are incorporated to: simplify assembly; eliminate "unnatural" or forced distortion of the collar/coil shape during yoke assembly and cooldown; and provide a rigid support to the collars/coil to resist Lorentz forces.

The philosophy of this yoke design is described as follows: The steel yoke lamination and aluminum spacer bar are dimensioned in such a way that the yoke has a nominal gap at the vertical split when assembled at room temperature. During assembly the 5/16" stainless steel shell is welded around the yoke and spacer bar and the shell stress rises to the yield strength of the shell material, around 30,000 psi.; after welding, the yoke gap has decreased, due to pressure from the shell, to a gap that is accurately controlled by the spacer bar. The collar and yoke profiles are dimensioned in such a way that the collar contacts the yoke at the horizontal diameter. Since the horizontal diameter of the collared coil assembly may vary slightly, the contact force due to the yoke along the side of the collar may also vary slightly; more for larger than average collars and less for smaller than average collars; however, the contact force between collar and yoke is maintained to remain greater than a predetermined minimum. During cooldown, the shell stress will increase; part way through cooling to 4 K the yoke gap will close. When fully cold, the gap is firmly closed and both the yoke gap and the spacer bar are firmly preloaded by the shell hoop force. During cooldown, the yoke maintains contact with the collar at the horizontal diameter. During excitation, most of the horizontal Lorentz forces appear on the yoke (the collar has a much smaller stiffness than the yoke ); although the load sharing between the yoke gap and spacer bar will shift, both will remain firmly loaded. As long as these two interfaces do not gap open the yoke will have good rigidity and minimal deflection due to coil excitation.

A 2-D model of the proposed yoke, spacer, and shell was constructed using the ANSYS Finite Element Program and is described in Ref. 2. The FEA mesh used in the analysis is shown in Fig. 3. Sliding elements were used to permit frictionless sliding and transmission of normal forces across closed gaps. Appropriate thermal contraction coefficients were used to produce stress changes during cooldown. Three different starting nominal yoke gaps, 8, 12, and 16 mils were used and the warm, cold, and excited conditions were determined for each starting case. Some selected observations from the analysis are given below.

1. During warm assembly the yoke gap decreases from the nominal by about .006 in. in all cases due to weld shrinkage.

2. After cooldown:

- a. The shell load approximately doubles in all cases because it contracts relatively more than the iron yoke when cooled.
- b. Both the spacer bar and yoke gap are closed and preloaded in all cases. The sharing of compression load between spacer bar and yoke depends upon the starting yoke gap used. The smaller the starting gap, the greater the yoke load will be relative to the spacer bar load.
- c. The inner diameter of the yoke at the midplane will decrease a precisely controlled amount determined by spacer bar dimensions; for this design example, the spacer bar width was chosen equal to the collar O.D.

3. During excitation:

- a. For 8 mil and 12 mil gaps, the yoke gap load decreases and the spacer bar load increases.
- b. The gap opens only slightly (.0001 - .0002) over a small area for the 8 and 12 mil cases; for the 16 mil gap, the yoke load after cooldown is not enough to keep the gap from opening excessively (.002 in.) when coil loads are applied.

The optimum starting nominal yoke gap is probably between 8 and 12 mils. For these cases adequate preload reserve exists on the spacer bar and yoke gap after cooldown to insure neither will lose contact during excitation. Perhaps some biasing toward the 8 mil case would be helpful in anticipating magnet operation at high field level; for this case, the yoke inside diameter decreases more than the collar by about .005 in. during cooldown and this excess yoke contraction guarantees good horizontal contact between yoke and collar after cooldown.

From the analysis, it appears that vertical split yoke with a spacer bar is sound and accomplishes the objectives of simplification of yoke assembly, preventing unnatural collar distortion after assembly or cooldown, and rigid support of the collar during excitation. Further analysis is warranted when more is known about interface friction, collar rigidity, and prestress due to welding of the shell.

### Cost Comparison

Fig. 4 shows the proposed 5 cm design together with the present 4 cm SSC design. Table IV lists the materials cost of the major components of the "cold mass" taken from the Conceptual Design Report<sup>5)</sup>, the cross sectional areas of these components for both the 4 cm and 5 cm designs, and a cost comparison. The cost of the materials will be approximately proportional to these areas; however, labor, tooling, etc., should be identical for the two designs.

Table IV - Comparison of 4 cm and 5 cm Costs

Components	WBS Item No.	Cost of Materials (M\$)	Area 4 cm Design (In <sup>2</sup> )	Area 5 cm Design (In <sup>2</sup> )	% Increase	Cost Increase (M\$)
Cable	.1.2.1.2.1.2.1	222	4.11	5.77	40.4	89.6
Collar Packs	.1.2.1.2.1.3.1	48	8.58	14.84	73.0	35.0
Yoke Laminations	.1.2.1.2.2.1.1	78	61.55	92.52	50.3	39.2
Shell	.1.2.1.2.2.2	23	6.69	12.89	92.7	21.3
Total Material cost		371				185.1
A1 spacer bar(not included in 4 cm design)						5.5
						190.7

Total Increase = 191 M\$

Increase in cryostat cost has not been studied, but should be small compared to that of the cold mass .

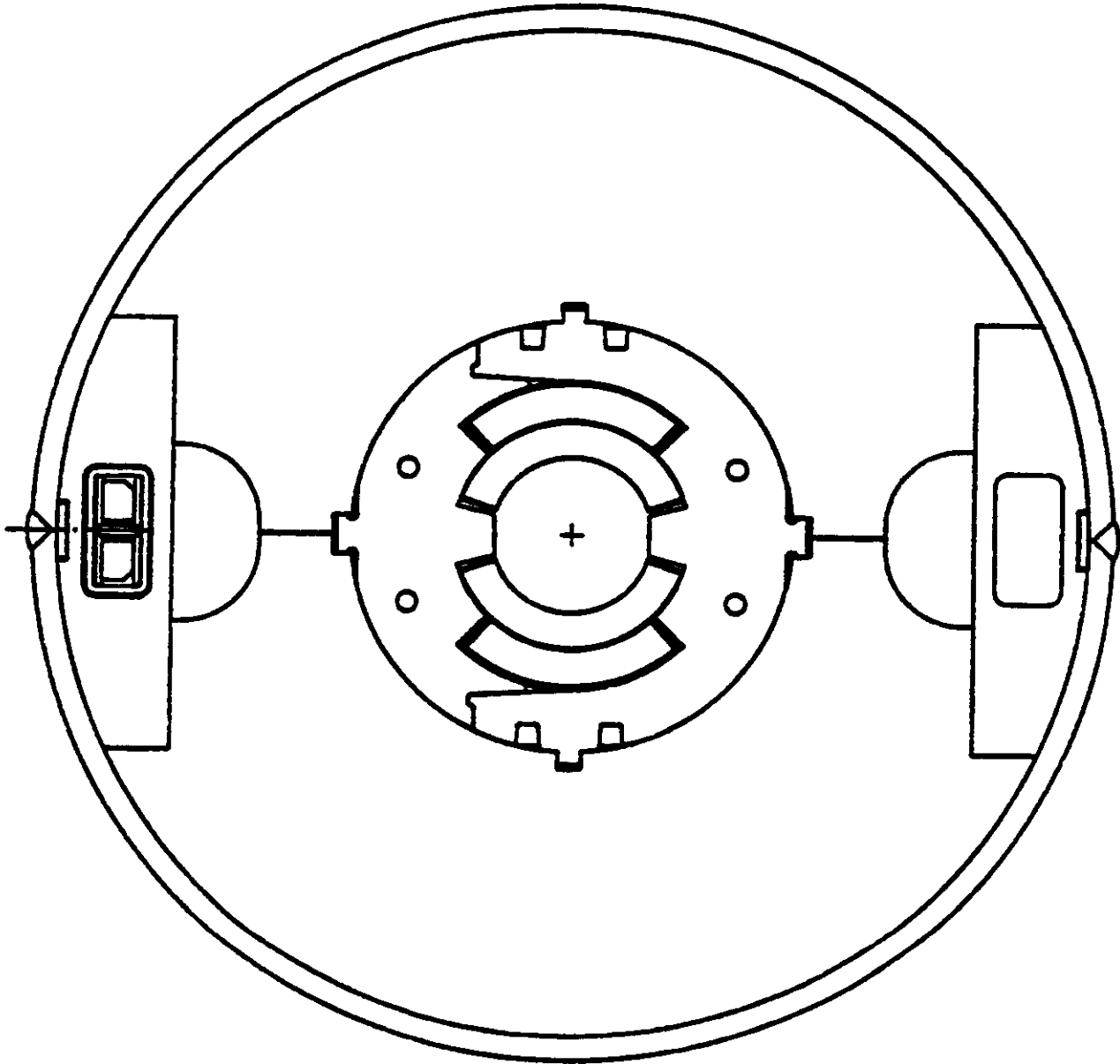
The increase is 191M\$; The largest component increase is 40% in cable cost or 90M\$ of which half (or 45M\$) is to increase the operating margin of safety in addition to the larger bore. These costs represent approx. 6.3% of the total CDR project cost of 3,010M\$. Of course, there will be small increases in several other costs because of the larger dipole mass and size; however, the listed costs should account for the major part of the increase.

### Conclusion

A 5 cm bore 6.6T design has been made which preserves the basic features and assembly methods developed for the present 4 cm design; this should help insure minimum development costs. In particular, the superconducting strand specification is preserved, but 20% more strands have been added to the cable to increase the operating margin of safety. Other minor features are proposed to improve the collar and yoke design and to simplify assembly. Because more materials are used, the cost of the collider magnets would increase by about 200M\$. A more detailed optimization study should be made if this type of magnet design is to be considered further.

### References

1. C. Taylor and S. Caspi, "Design of a 9T 5 cm Bore Dipole", SSC-MAG-207, LBID-1418, July 1, 1988.
2. C. Peters, "Description and Analysis of 5 cm Vertically Split Yoke Design", SSC-MAG-235, March 22, 1989.
3. C. Taylor, S. Caspi, M. Helm, K. Mirk, C. Peters, and A. Wandesforde, "A High Gradient Quadrupole Magnet for the SSC", presented at the 1987 Particle Accelerator Conference, Washington, DC, March 16-19, 1987.
4. D. Leroy, M. Castiglioni, and D. Hagedorn, "A 5 m Long Impregnated NbTi Dipole Magnet", published in the *IEEE Trans. on Nucl. Sci.*, Vol. NS-32, No. 5, October 1985.
5. SSC Conceptual Design Report - Attachment D, SSC-SR-2020D, March 1986.



PROPOSED D16x CROSS SECTION (4/21)

Fig. 1

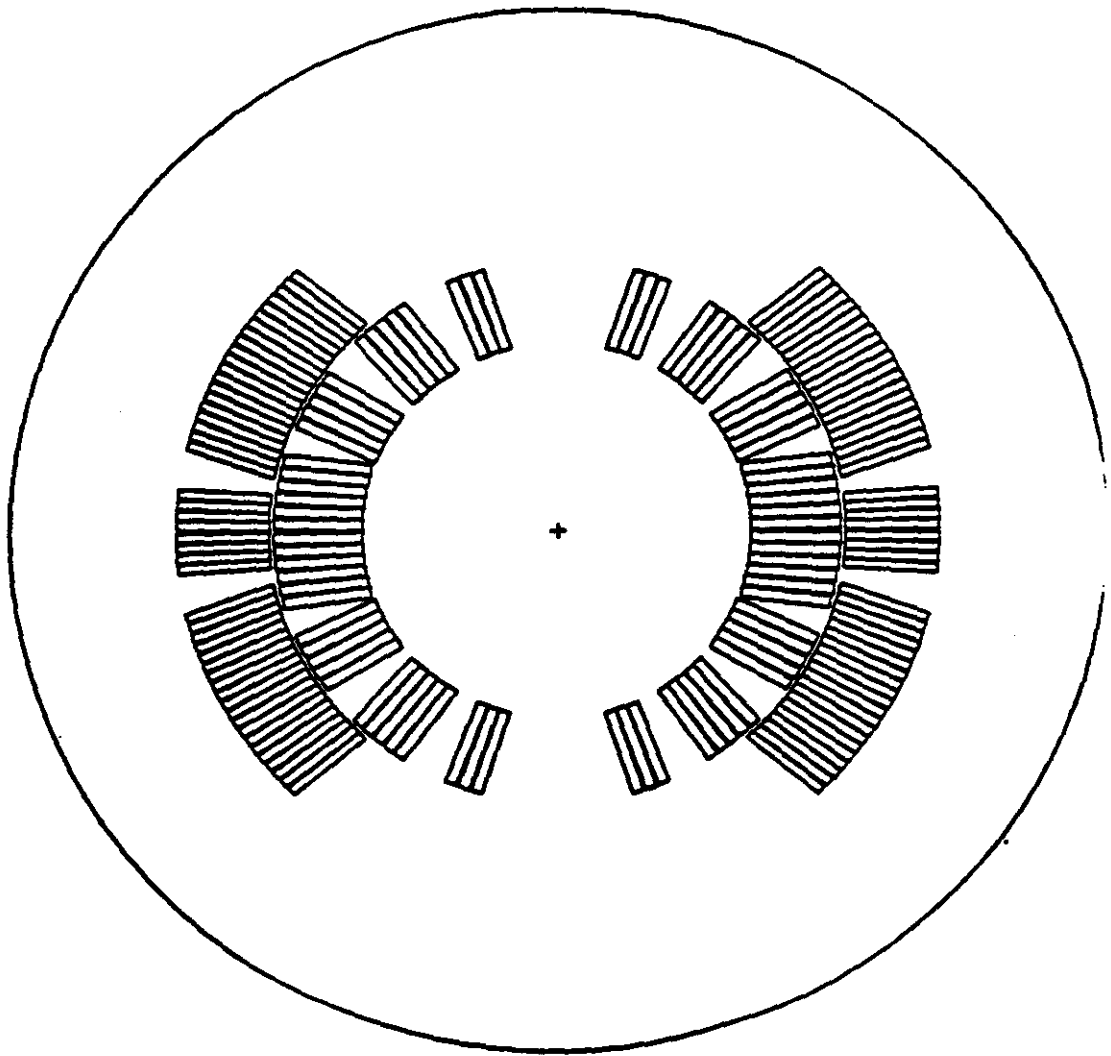
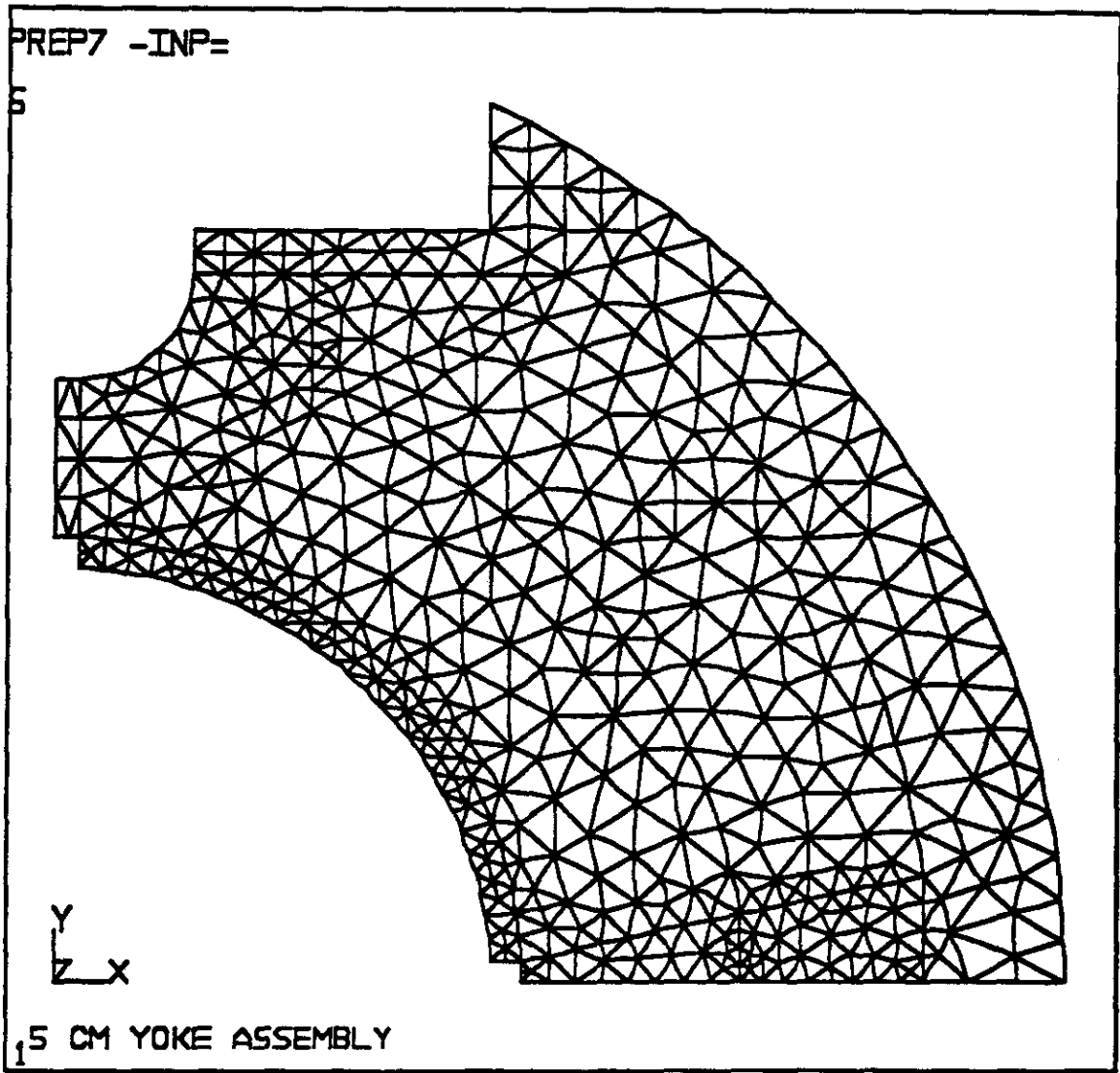


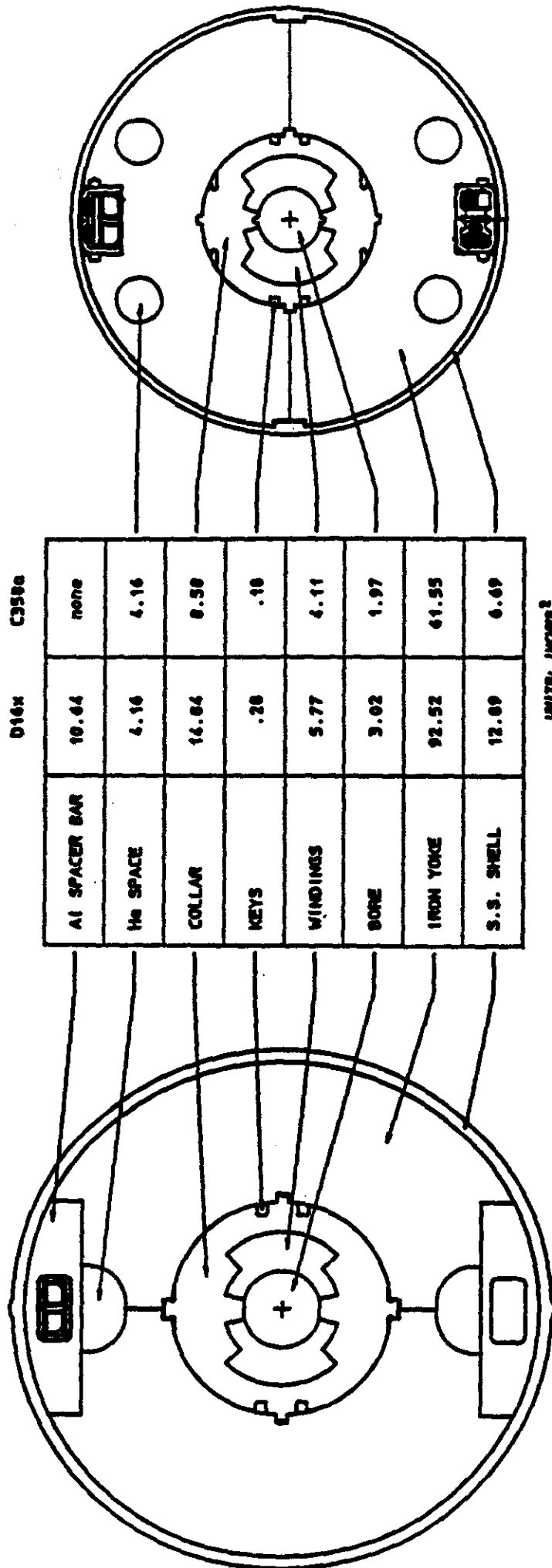
Fig. 2



MAR 28 1989  
PREP7 ELEMENT  
ZK=1  
DIST=3.54  
X=2.52

Fig. 3

CROSS SECTIONAL AREA COMPARISON : D16x VS C350a



D16x SECTION  
5 CM BORE

C350a SECTION  
4 CM BORE

Fig. 4

## APPENDIX A

### Comparison of Operating "Margin"

A comparison of calculated operating margin for the 4 cm present design and the 5 cm (D16X) design presented here is given in Table AI. For the 4 cm design the transfer function and saturation behavior is taken from Morgan<sup>1)</sup> for C358A; similar values are given by Caspi<sup>2)</sup> for NC-9. For the 5 cm D16X design, since "real"  $\mu$  calculations have not yet been done, the  $\mu = \infty$  transfer function is assumed to vary with field in a way that is proportional to the 4 cm transfer function calculated by Morgan. This should be quite accurate since the two designs are geometrically similar. The critical current is the SSC specified minimum of 7860A for Cu/SC = 1.3 and 7231A for Cu/SC = 1.5 at 7.0T, 4.2K, for the 23 strand inner cable,<sup>3)</sup> increased by the factor 28/23 for "5 cm". For variation of current with B and T we use the simple linear relationships given in<sup>3)</sup> since extrapolation from 7.0T and 4.2K is small. Operating temperature of 4.35K is assumed.

For "4 cm" and Cu/SC = 1.3, maximum operating current  $I_c = 6.79\text{KA}$  at  $B_0 = 6.86\text{T}$  for a current margin of 4.5% (i.e.  $6.79\text{KA}/6.50\text{KA} = 1.045$ ); for "5 cm",  $I_c = 7.59\text{KA}$  at  $B_0 = 7.03\text{T}$  for current margin of 12.1% - an increase of a factor of 2.7 (i.e.  $12.1/4.5$ ). Another definition of margin that is sometimes used is the excess critical current at the design operating field of  $B_0 = 6.6\text{T}$ ; this value is also given in the table. Values are also given for Cu/SC = 1.5.

Calculations based on slight variations in cross-section design and cable current may change the values shown in Table AI, but will not change the relative margins significantly for the purpose of comparison.

1. G. Morgan, "C358A - A New SSC Dipole Coil and End Design", BNL, CDG-N-342, AD/SSC/Tech. No. 62, May 20, 1987.
2. S. Caspi and M. Helm, "The Load Line and Critical Current for the SSC Dipole Magnet with the NC9 Cross Section", SSC-MAG-168 Revised, LBID-1331, December 1, 1987.
3. R. Scanlan, "NbTi Superconductor Cable for SSC Dipole Magnets", Material Specification, SSC-MAG-M4142, Revision 3, 1/4/89.

Table I - Appendix

Design		SSC Operating Point					Current Margin at Magnet Plateau "Along Load Line"				Current Margin at $B_0 = 6.6T$	
		Cu/SC	$B_0$ (T)	$B_{max}$ (T)	$I_{op}$ $\mu = \infty$ (kA)	$I_{op}$ real $\mu$ (kA)	$B_0$ (T)	$B_{max}$ (T)	$I_c$ (kA)	$(1-I_c/I_{op})$ (Margin)	$I_c$ (kA)	$(1-I_c/I_{op})$ (Margin)
4 cm	1.3	6.60	6.93	6.35	6.50	6.86	7.20	6.79	4.5%	7.45	14.6%	
4 cm	1.5	6.60	6.93	6.35	6.50	6.71	7.04	6.61	1.5%	6.92	6.5%	
5 cm	1.3	6.60	6.90	6.62	6.77	7.03	7.43	7.59	12.1%	9.16	35.3%	
5 cm	1.5	6.60	6.90	6.62	6.77	6.93	7.27	7.41	9.4%	8.42	24.4%	